

Metal–Organic Frameworks

An Anionic Interpenetrated Zeolite-Like Metal–Organic Framework Composite As a Tunable Dual-Emission Luminescent Switch for Detecting Volatile Organic Molecules

Wei Xie,^[a] Wen-Wen He,^[a] Shun-Li Li,^[b] Kui-Zhan Shao,^[a] Zhong-Min Su,^{*,[a]} and Ya-Qian Lan^{*,[a, b]}

Abstract: The luminescent MOF $[(CH_3)_2NH_2]_2[(Zn_2O)L] \cdot 5 DMF$ (NENU-519, NENU = Northeast Normal University) with a zeolite BCT topology was successfully synthesized. It is a rare example of a two-fold interpenetrated framework with a zeolite topology. NENU-519 demonstrates the ability to selectively adsorb cationic dyes. Furthermore we developed Rh6@NENU-519 (Rh6 = Rhodamine 6G) as a dual-emitting sensor for probing different volatile organic molecules (VOMs) due to an energy transfer between L and the dye. The composite can be used to distinguish the isomers of *o*-, *m*-, and *p*-xylene and ethylbenzene using the emission-peak-

height ratios of L to the dye as detectable signals, in which the readout signals are involved in the interactions between the dye@MOF composite and the guest analytes. Moreover, Rh6@NENU-519 can serve as a luminescent switch for the detection of different aromatic compounds, like benzene, benzene substituted with different groups, and pyridine. In other words, the Rh6@NENU-519 composite can be used as molecular decoder of the structural information of different VOMs into recognizable luminescent signals. Hopefully this work will open a new corridor to develop luminescent guest@MOF composites as sensors for practical applications.

Introduction

Metal–organic frameworks (MOFs) have evoked great interest due to their aesthetically captivating structures and intriguing potential applications in various fields of gas storage, separation, chemical sensing, imaging, heterogeneous catalysis, and drug delivery.^[1–4] More desirably, the crystal engineering of MOFs is a long-standing challenge in control of the network topology. Particularly, zeolite networks are very important topologies for the production of porous materials. However, obtaining MOFs with zeolite topologies is still difficult and challenging, because tetrahedral SBUs (secondary building units) are prone to assemble into the diamond (dia) topology.^[5a] Zeolite networks are relatively scarce porous MOFs, although some MOFs with zeolite topologies (such as MTN,^[5b,c] SOD,^[5d] ABW,^[5e] and NPO^[5f]) have been reported. These observations inspire us to attempt to generate MOFs with zeolite topologies.

The inorganic and organic moieties in MOFs can directly generate luminescence that can be used in chemical sensors.^[6] Furthermore, the tunable pore size and shape of MOFs impart them with the capability to accommodate guest luminophore molecules into their cavities, offering another degree of diversity of their luminescent properties.^[7] Therefore, MOFs as luminescent sensing materials have attracted great attention and are widely explored by researchers.^[8] The rapid, reliable, and efficient detection of volatile organic molecules (VOMs) is a very significant subject for environmental and health issues.^[9] Moreover, the majority of these VOMs possess similar structures and properties, such as isomers, which makes the probing of different VOMs with clearly differentiable and unique readouts still a critical challenge.^[10] Distinguishing subtle distinctions in molecules requires chemosensors that can selectively recognize specific molecules and then transduce the recognitions into detectable signals. Porous MOFs generally have guest-dependent optical properties and, therefore, have the potential to recognize target molecules through the unique host–guest interaction. However, most luminescent sensors explored so far are limited to a fluorescence signal of one transition, which is not accurate enough because the absolute single-emission intensity varies depending on many uncontrollable factors.^[11] Therefore, a new dual-emission strategy to increase the sensing selectivity can be envisioned by producing MOFs as hosts to encapsulate chromophore guests. However, it is a significant but challenging task to design suitable luminescent MOF composites as dual-emitting systems in response to guest–host interactions.

[a] Dr. W. Xie, Dr. W.-W. He, Dr. K.-Z. Shao, Prof. Z.-M. Su, Prof. Y.-Q. Lan
Institute of Functional Material Chemistry, Faculty of Chemistry
Northeast Normal University, Changchun, 130024 Jilin (P. R. China)
E-mail: zmsu@nenu.edu.cn

[b] Prof. S.-L. Li, Prof. Y.-Q. Lan
Jiangsu Key Laboratory of Biofunctional Materials
School of Chemistry and Materials Science
Nanjing Normal University, Nanjing, 210023, Jiangsu (P. R. China)
E-mail: yqlan@njnu.edu.cn

Supporting information for this article is available on the WWW under <http://dx.doi.org/10.1002/chem.201603487>.

Fluorescent dyes can be used as chromophore guests owing to their excellent optical and electronic properties and high quantum yield. Applications of MOFs for dye adsorption and separation have been extensively explored.^[12] Therefore, it will be feasible to construct luminescent MOF composites that contain fluorescent dyes for fluorescence applications. Dye@MOF composites as dual-emission systems for luminescent sensing have rarely been reported.^[13] Previously, Wu et al. established a luminescent dye@MOF platform for the fingerprint sensing of VOMs based on two different emissions.^[13a] Our group used a dye@MOF as a dual-emitting fluorescent sensor for sensing explosives.^[13b] Therefore, the composites should be very promising luminescent materials for practical applications. In addition, cationic fluorescent dyes would not be released from the pores of anionic MOFs due to the strong electrostatic interactions between the anionic framework and cationic dyes. Furthermore, the MOF/dye approach is an important and feasible strategy to construct MOF composites for diverse applications. Previously, such a strategy has been implemented to develop nonlinear optical (NLO) and laser materials.^[14]

Herein, we report a novel luminescent MOF with a zeolite BCT topology, namely $[(\text{CH}_3)_2\text{NH}_2]_2[(\text{Zn}_2\text{O})\text{L}]\cdot 5\text{DMF}$ (NENU-519, NENU = Northeast Normal University), based on the carboxylates ligand tetrakis[4-(carboxyphenyl)oxamethyl]methane acid (H_4L) (Figure S1 and S2 in the Supporting Information). It is an interpenetrated framework with a zeolite topology, a class which has rarely been reported. The anionic framework can be used to selectively separate cationic dyes based on ionic interactions rather than the size-exclusion effect. More importantly, the Rh6@NENU-519 composite was explored as a dual-emitting luminescent platform to distinguish the isomers of *o*-, *m*-, and *p*-xylene and ethylbenzene, which only have subtle differences in their structures, based on the emission-peak-height ratios of L and the dye moieties. Therefore, Rh6@NENU-519 can be used as a tunable dual-emitting luminescent switch for the detection of different aromatic compounds, like benzene, benzene substituted with different groups, and pyridine, which are involved in the tuning of the energy transfer efficiency from the MOF to the dye.

Results and Discussion

Single crystal X-ray diffraction analysis reveals that NENU-519 crystallizes in the tetragonal space group $\bar{P}4n2$ (Table S1). The asymmetric unit contains two Zn ions and one deprotonated L^{4-} ligand. Zn1 is coordinated by four carboxylate oxygen atoms from the L^{4-} ligand in a tetrahedral geometry. Zn2 also adopts a tetrahedral coordination with three carboxylate groups from the L^{4-} ligand and one terminally coordinated water molecule (Figure S3). The bond lengths of the Zn–O bonds are all within the normal ranges.^[15] The SBUs of NENU-519 are 4- and 6-rings of binuclear Zn clusters linked by L^{4-} fragments, from which the subunits of the 4^26^4 cages (16.2 Å in diameter) are constructed (Figure 1 a). These cages connect with each other into a 3D anionic network (Figure 1 b). The structure is characterized by two sets of channels build by

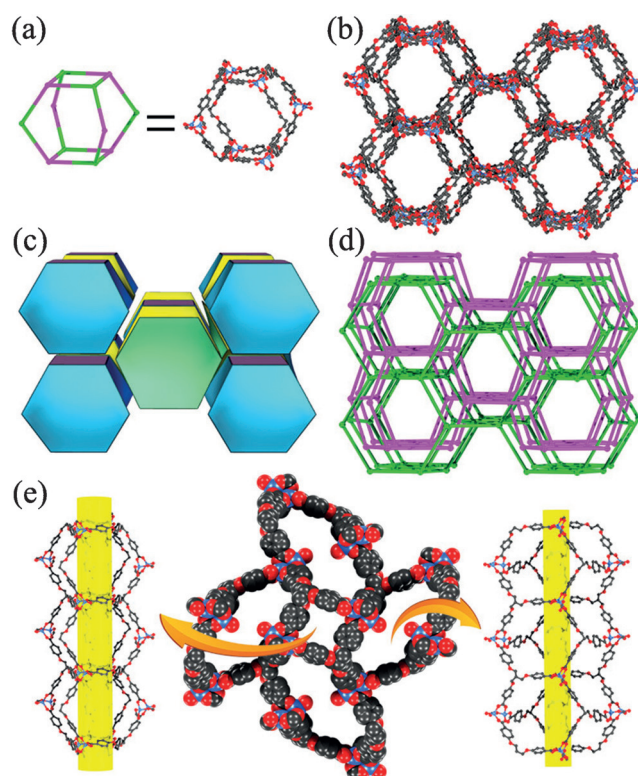


Figure 1. Different structure models of $[(\text{CH}_3)_2\text{NH}_2]_2[(\text{Zn}_2\text{O})\text{L}]\cdot 5\text{DMF}$ (NENU-519, NENU = Northeast Normal University): a) Representation of a single cage and b) the ball-and-stick representation of the 3D structure in NENU-519; c) The zeolite-like BCT (or crb) net is shown as a tiling diagram; d) The ball-and-stick representation of the 2-fold interpenetrating open framework; e) Space-filling model of one layer along the *c* axis (middle) and the two different channels in NENU-519 (left and right).

chains of 4^26^4 cages of 14.37×15.19 Å and an elliptical 8-ring opening of 25.09×6.49 Å along the *c* axis (Figure 1 e, Figure S4 and S5 in the Supporting Information). The topology of NENU-519 can be rationalized as *s* zeolite BCT (or named as *crb*) structure by regarding dinuclear Zn clusters and tetratopic ligands as 4-connected building units (Figure 1 c and Figure S4 in the Supporting Information), which is rarely found in MOFs,^[16] because the tetrahedral nodes are generally assembled into diamond or quartz nets. Notably, such two nets interlock together to generate a 2-fold interpenetrating framework (Figure 1 d and Figure S5 in the Supporting Information), which is a rare example of an interpenetrated framework reported for zeolite-like MOFs.^[5f] Through interpenetrating, the effective free volume of NENU-519 was calculated by PLATON^[17] and the calculations indicate that the effective free volume is about 62.7% of the crystal volume (8750 Å³ of the 13964 Å³ unit cell volumes). The solvent molecules and $[(\text{CH}_3)_2\text{NH}_2]^+$ cations originated from decarbonylation of dimethylamine, reside in the channels.

Now organic dyes are widely employed in paper, plastics, printing, textile, cosmetics, and other industries. From environmental and health points of view, removing organic dyes from effluents before discharging is vitally important. So we tried to evaluate the absorption abilities of the zeolite-like NENU-519 towards dye molecules with different charges and sizes. We se-

lected four cationic dyes (methylene blue (MB), Basic Red 2 (BR), rhodamine 6G (Rh6), and crystal violet (CV)), four anionic dyes (methyl orange (MO), fuchsin acid (FA), Brilliant Blue R-250 (R-250), and congo red (CR)), and two neutral dyes (Solvent Yellow 2 (SY) and methyl red (MR)) (Figure S7). After the as-synthesized NENU-519 samples have been soaked in DMF solutions of the dyes for a period of time, different adsorption behaviors can simply be observed by the naked eye. The cationic dyes (MB, BR, Rh6, and CV) could be efficiently adsorbed and the colorless crystals became gradually colored, whereas the anionic and neutral dyes (MO, FA, R-250, CR, SY, and MR) could not be adsorbed (Figure S8 and Table S2). The PXRD patterns and FT-IR profiles of the dye@MOFs suggested that the crystallites remained intact after exchange of the cationic dyes (Figure S9 and S10). The selective absorption of cationic dyes could be explained by an exchange of the $[(CH_3)_2NH_2]^+$ cations with the cationic dyes within the anionic framework.

As another factor, the size of the dyes may influence the ion exchange process. The exchange process of the four cationic dyes with an equal charge ($Z = +1$) but different sizes in the supernatant was monitored by UV/Vis absorption spectroscopy (Figure S11). The ion exchange of MB was complete in 3 h, the larger-sized BR after 6 h, but crystal violet (CV) and rhodamine 6G (Rh6) needed more time using the same concentration ($1 \times 10^{-5} \text{ mol L}^{-1}$). With increasing size of the cationic dyes, the ion-exchange process became slower. In other words, the size of the cationic dyes is also another contributing factor in the ion-exchange process.

Furthermore, we used NENU-519 to separate cationic dyes from dye mixtures. Typically, the freshly prepared NENU-519 was immersed in DMF solutions of MB/MO, BR/R-250, and CV/SY. The cationic dyes (i.e., MB, BR, and CV) could be adsorbed from the dye mixtures followed by a color change of the solutions (Figure 2), while the anionic (MO and R-250) and neutral (SY) dyes could not be adsorbed and remained in the supernatants. So the results indicate that NENU-519 could be used to selectively absorb cationic dyes from dye mixtures and as potential absorbents to remove cationic dyes from effluents.

Furthermore, dye releasing experiments were performed in order to confirm whether the selective absorption is attributed to ionic interactions of the cationic dyes with the anionic

framework. The release processes were monitored by UV/Vis spectroscopy in pure DMF and saturated solutions of NaCl in DMF.^[18] The results showed that in the presence of NaCl the cationic dyes were gradually released, while in pure DMF without NaCl the dye molecules were hardly released (Figure S12). Hence, we can safely conclude that selective absorption is due to the interaction of the cationic dyes with the anionic framework. In addition, the reversible ion-exchange process for methylene blue was studied for five continuous cycles. PXRD demonstrated that the crystalline integrity of NENU-519 could be kept after five cycles of exchange–release processes (Figure S13).

The successful encapsulation of fluorescent dyes into MOFs provides the basis to explore their application as fluorescence sensors. The rhodamine 6G fluorescent dye has been successfully encapsulated into the channels of NENU-519 as mentioned above, which prompts us to explore the fluorescent properties of Rh6@NENU-519 in detail. The luminescent properties of free H₄L and NENU-519 were examined at room temperature in the solid state. Compared with the free H₄L ligand, NENU-519 exhibited an obvious enhanced blue emission with a maximum at 406 nm, which is attributed to the deprotonation and the coordination of L to Zn²⁺ ions (Figure S15).^[19] As expected, the emission spectra of Rh6@NENU-519 simultaneously exhibited two characteristic emissions upon excitation at 350 nm in the solid state at room temperature. The blue emission at 406 nm is attributed to L, whereas the new red emission at about 565 nm originated from Rh6 (Figure S17). As a comparison, we also studied the fluorescent properties of Rh6 and a thoroughly ground mixture of NENU-519 and Rh6 under the same conditions. Rh6 did not show any emission in the solid state, whereas the DMF solution of Rh6 displayed an emission at 564 nm (Figure S16). The finely ground mixture only presented the emission band of pure NENU-519 (Figure S17). These results indicated that the dye molecules were enclosed into the channels of NENU-519, which can restrain the nonradiative energy transfer process.^[13] Furthermore, after soaking of Rh6@NENU-519 (10 mg) in DMF (10 mL) for one day, no obvious emission bands have been observed in the emission spectrum of the filtrate (Figure S18). The result further demonstrates that the dye Rh6 was not released from the

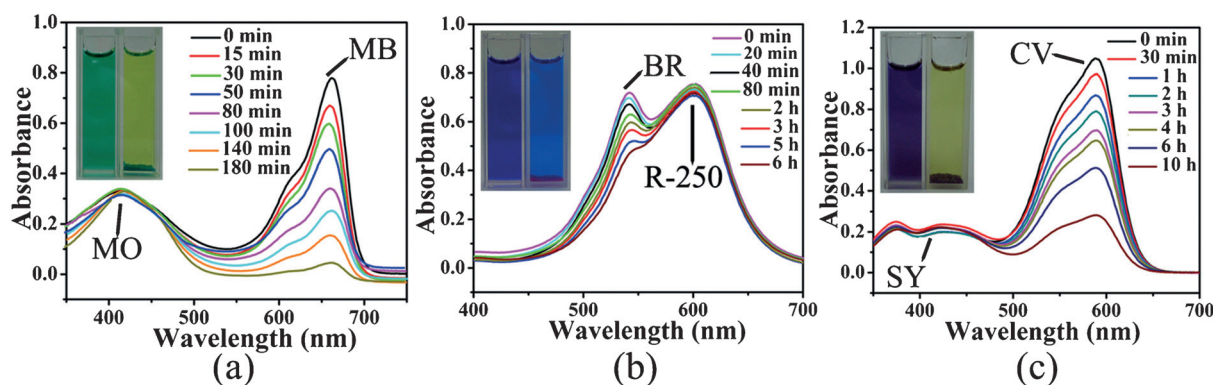


Figure 2. UV/Vis spectra and photographs of DMF solutions of different dyes with NENU-519: a) Methylene blue (MB)/methyl orange (MO), b) Basic Red 2 (BR)/Brilliant Blue R-250 (R-250), and c) crystal violet (CV)/Solvent Yellow 2 (SY).

pores of the MOF due to the strong electrostatic interactions between the anionic framework of NENU-519 and the cationic dye rhodamine 6G.

The luminescence of Rh6@NENU-519 inspired us to systematically tune the emission of this system by adjusting the amounts of the encapsulated Rh6. By varying the immersing time, a series of Rh6@NENU-519-a-g could be conveniently obtained. The contents of the included Rh6 in Rh6@NENU-519-a-g were determined by UV/Vis absorption spectroscopy to be 0.012 wt%, 0.029 wt%, 0.051 wt%, 0.076 wt%, 0.098 wt%, 0.127 wt%, 0.158 wt% for a-g, respectively (Figure S14). As shown in Figure 3, upon increasing the Rh6 content, the emission intensity of the dye at 565 nm steadily increased, whereas the intensity of the L at 406 nm decreased correspondingly. This system exhibited a tunable luminescent emissions controlled by adjusting the transition-intensity ratios between L and the dye. The corresponding CIE (Commission International de l'Eclairage) coordinates of Rh6@NENU-519-a-g, which can be directly and clearly observed with the naked eye under a 365 nm UV light (Figure 3-c and 3d), were marked. The emission of Rh6 in Rh6@NENU-519 is probably due to the sensitiza-

tion of the L within the same framework. Such a L-to-dye-energy-transfer behavior can be confirmed by the overlap between the emission spectrum of the MOF and the UV/Vis absorption spectrum of the dye (Figure S19). In addition, the quantum yield of 22.1% for Rh6@NENU-519g was higher than that of NENU-519 (5.7%) excited at 350 nm. The above results clearly indicate that the luminescence of Rh6@NENU-519 and the L-to-dye energy transfer depend on the content of the encapsulated rhodamine 6G.

The isomers of *o*-, *m*-, and *p*-xylene and ethylbenzene have subtle differences of their structures and very similar structural motifs, so it is a critical and challenging task to distinguish these isomers in environmental monitoring by a specifically designed molecular sensor. Considering that the emission intensities of the MOF and dye are comparable, we explored the sensing capability of Rh6@NENU-519-e for probing these isomers. After samples of Rh6@NENU-519-e were exposed to *o*-, *m*-, and *p*-xylene and ethylbenzene solvents, the photoluminescence spectra showed emission peaks central around the 406 and 565 nm transitions (Figure 4a). Although the single emissive intensity of MOF or dye is nonspecific to these sol-

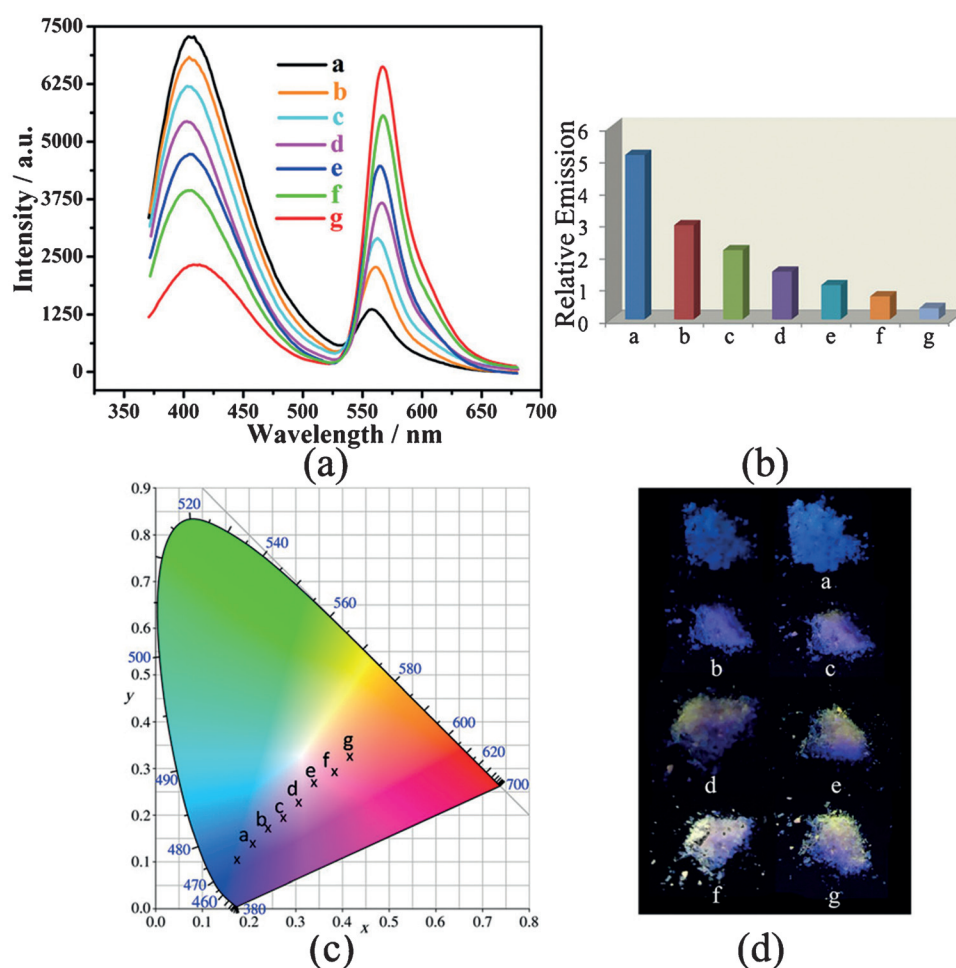


Figure 3. The fluorescent properties of Rh6@NENU-519 (Rh6 = Rhodamine 6G; Rh6 concentration: a = 0.012 wt%, b = 0.029 wt%, c = 0.051 wt%, d = 0.076 wt%, e = 0.098 wt%, f = 0.127 wt%, and g = 0.158 wt%): a) The emission spectra excited at 350 nm in the solid state at room temperature; b) The corresponding emission peak-height ratios of L to the dye moieties; c) The corresponding CIE chromaticity coordinates; d) The corresponding photographs under a laboratory 365 nm UV light.

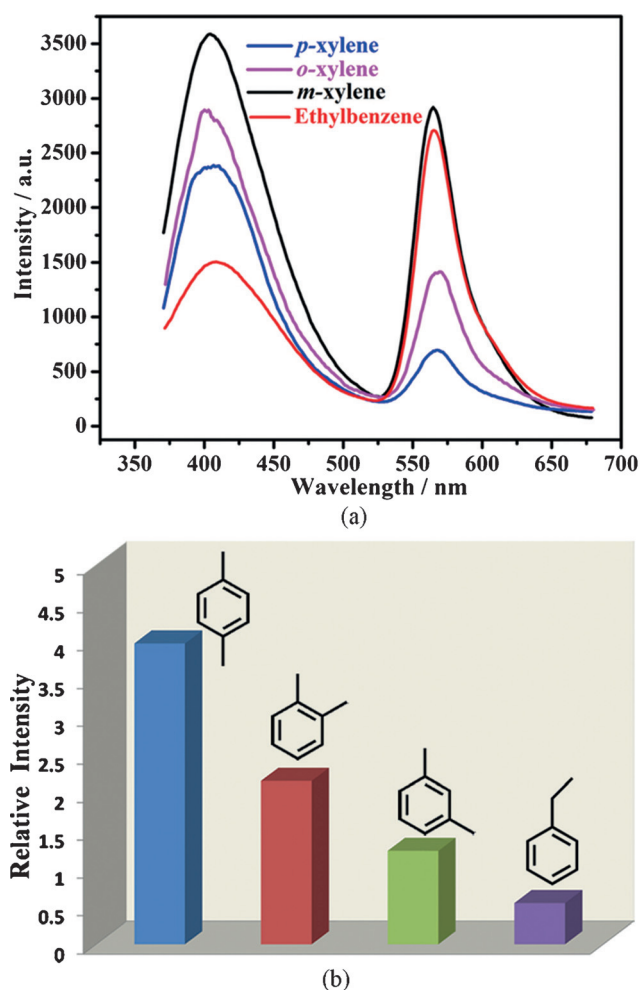


Figure 4. a) The emission spectra of Rh6@NENU-519-e dispersed in *m*-xylene, *o*-xylene, *p*-xylene, and ethylbenzene excited at 350 nm at room temperature. b) The corresponding solvent-dependent emission peak-height ratios of L to the dye in the luminescence spectra.

vents, these isomer molecules could be easily distinguished by monitoring the relative emission intensities of the L-to-dye moieties. The peak-height ratios of L and dye are 3.96 for *p*-xylene, 2.15 for *o*-xylene, 1.23 for *m*-xylene, and 0.54 for ethylbenzene (Figure 4b). We think that the interaction of the guest molecules and Rh6@NENU-519-e will influence the energy transfer efficiency between L and the dye. The key to success in distinguishing the isomers of *o*-, *m*-, and *p*-xylene and ethylbenzene is to use the dual-emission peak-height ratios of L and the dye moieties as detectable signals by self-calibrating the energy transfer behaviors.

Such a dual-emitting luminescent sensor for distinguishing the isomers of *o*-, *m*-, and *p*-xylene and ethylbenzene is remarkable, because it was very sensitive to different isomer molecules and required no additional calibration. The peak-height ratios of L to the dye moieties were variable to different isomers, but the ratio was almost a constant and unique for each guest. In other words, Rh6@NENU-519-e can be used for distinguishing isomers by simply monitoring the relative emission intensities. Such a ratiometric luminescent sensor of

Rh6@NENU-519-e demonstrated selective solvent-responsive changes, which can be attributed to the interaction between guest molecules and the host composite having different effects on the energy-transfer efficiency from L to the dye.

Furthermore, we use Rh6@NENU-519-e to detect the VOMs benzene, benzene substituted with different groups, and pyridine. The Rh6@NENU-519-e samples were immersed into benzene, toluene, phenol, chlorobenzene, bromobenzene, and pyridine, and the emission peak-height ratios of L to the dye moieties were also dependent on the VOMs used. These VOMs could be unambiguously distinguished by monitoring the peak-height ratios, which can be rationalized by the unique guest-dependent energy transfer from L to the dye (Figure 5). Although the luminescent emission intensities of Rh6@NENU-519-e were significantly quenched by nitrobenzene and aniline, they still could be differentiated clearly in low concentration (50 ppm DMF solutions) due to their different influences on the energy-transfer process (Figure S20). Additionally, the sensing stability of the Rh6@NENU-519-e sensor was confirmed by recycling experiments. The emission-peak-height ratio of L to the dye remained nearly the same for five cycles in sensing benzene molecules (Figure S21). The framework of NENU-519 still remained intact after five recycling experiments, as confirmed by PXRD (Figure S22).

This molecular decoding strategy using dual emission is strongly correlated with the interactions between the

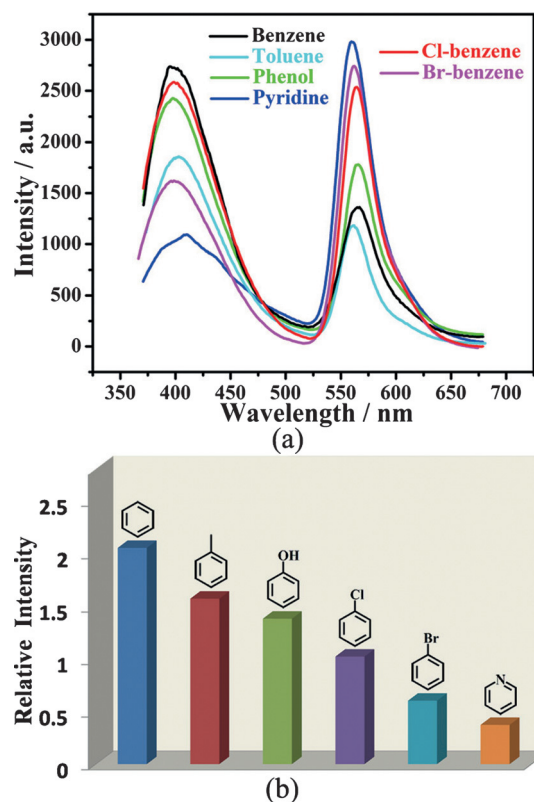


Figure 5. a) The emission spectra of Rh6@NENU-519-e dispersed in benzene, toluene, phenol, Cl-benzene, Br-benzene, and pyridine excited at 350 nm at room temperature. b) The corresponding solvent-dependent emission peak-height ratios of L to the dye in the spectra.

Rh6@NENU-519 composite and the guest analytes. The dual emission of Rh6@NENU-519-e contributed to the decoding system, because it can differentially recognize different VOMs and transcribe the recognition into detectable signals. The Rh6@NENU-519-e composite can be used as tunable luminescent switch towards VOMs with corresponding relative emission intensities as signals by modulating the energy transfer from L to the dye. This approach exhibited a plain distinguishable emission for each VOM, thus an emission-fingerprint map for sensing VOMs can be drawn based on the peak-height ratios of two emissions in Rh6@NENU-519-e. The ratiometric internal-reference sensor could overcome the drawback of variability encountered of a single absolute emission intensity.

Conclusion

In summary, a novel anionic luminescent MOF with a zeolite BCT topology has been constructed. It is a rare example of an interpenetrated MOF based on the zeolite topology. The MOF was used to selectively absorb and separate cationic dyes based on a charge- and size-dependent ion-exchange process. More importantly, we developed a luminescent dye@MOF sensor for probing different VOMs based on the two emissions of MOF and dye. The dual-emitting luminescent sensor was used to reliably distinguish the isomers of *o*-, *m*-, and *p*-xylene and ethylbenzene, and it can be used as a luminescent tunable switch towards different aromatic compounds, like benzene, benzene substituted with different groups, and pyridine. Such a molecular assemble can decode structural information of VOMs into a corresponding fluorescent signals. The Rh6@NENU-519 sensor exhibited a high sensitivity due to the excellent fingerprint correlation between the VOMs and the relative emission intensities of two different moieties by tuning the energy-transfer efficiency. Because of its instantaneous, and stable self-calibration, this very promising luminescent dual-emitting dye@MOF sensor has potential applications in ratiometric luminescent sensors for probing different substrate molecules/ions.

Supporting information for this article is given via a link at the end of the document, including experimental details, crystal data (CCDC 1465369)^[20], structural information, PXRD, IR, TGA data, fluorescence measurements, and additional figures.

Acknowledgements

This work was financially supported by the National Natural Science Foundation of China (No. 21371099, 21401021, and 21471080), the NSF of the Jiangsu Province of China (No. BK20130043 and BK20141445), the Priority Academic Program Development of the Jiangsu Higher Education Institutions, and the Foundation of the Jiangsu Collaborative Innovation Center of Biomedical Functional Materials.

Keywords: cationic dyes · dual-emitting luminescent sensors · metal-organic frameworks · volatile organic molecules · zeolites

- [1] a) J. R. Long, O. M. Yaghi, *Chem. Soc. Rev.* **2009**, *38*, 1213–1214; b) H. C. Zhou, J. R. Long, O. M. Yaghi, *Chem. Rev.* **2012**, *112*, 673–674; c) Z. Hu, B. J. Deibert, J. Li, *Chem. Soc. Rev.* **2014**, *43*, 5815–5840; d) J. A. Mason, M. Veenstra, J. R. Long, *Chem. Sci.* **2014**, *5*, 32–51; e) P. Horcjada, R. Gref, T. Baati, P. K. Allan, G. Maurin, P. Couvreur, G. Férey, R. E. Morris, C. Serre, *Chem. Rev.* **2012**, *112*, 1232–1268.
- [2] a) G. Férey, C. Serre, T. Devic, G. Maurin, H. Jobic, P. L. Llewellyn, G. De Weireld, A. Vimont, M. Daturi, J. S. Chang, *Chem. Soc. Rev.* **2011**, *40*, 550–562; b) S. T. Zheng, T. Wu, C. Chou, A. Fuhr, P. Feng, X. Bu, *J. Am. Chem. Soc.* **2012**, *134*, 4517–4520; c) T. A. Makal, J. R. Li, W. Lu, H. C. Zhou, *Chem. Soc. Rev.* **2012**, *41*, 7761–7779; d) K. C. Stylianou, J. Rabone, S. Y. Chong, R. Heck, J. Armstrong, P. V. Wiper, K. E. Jelfs, S. Zlatogorsky, J. Bacsá, A. G. McLennan, C. P. Ireland, Y. Z. Khimyak, K. M. Thomas, D. Bradshaw, M. J. Rosseinsky, *J. Am. Chem. Soc.* **2012**, *134*, 20466–20478.
- [3] a) H. Wu, Q. Gong, D. H. Olson, J. Li, *Chem. Rev.* **2012**, *112*, 836–868; b) H. Deng, C. J. Doonan, H. Furukawa, R. B. Ferreira, J. Towne, C. B. Knobler, B. Wang, O. M. Yaghi, *Science* **2010**, *327*, 846–850; c) P. Nugent, Y. Belmabkhout, S. D. Burd, A. J. Cairns, R. Luebke, K. Forrest, T. Pham, S. Ma, B. Space, L. Wojtas, E. Mohamed, M. J. Zaworotko, *Nature* **2013**, *495*, 80–84.
- [4] a) S. Kim, K. W. Dawson, B. S. Gelfand, J. M. Taylor, G. K. H. Shimizu, *J. Am. Chem. Soc.* **2013**, *135*, 963–966; b) P. Wu, C. He, J. Wang, X. Peng, X. Li, Y. An, C. Duan, *J. Am. Chem. Soc.* **2012**, *134*, 14991–14999; c) G. Q. Kong, S. Ou, C. Zou, C. D. Wu, *J. Am. Chem. Soc.* **2012**, *134*, 19851–19857; d) W. Xie, S. R. Zhang, D. Y. Du, J. S. Qin, S. J. Bao, J. Z. M. Su, W. W. He, Q. Fu, Y. Q. Lan, *Inorg. Chem.* **2015**, *54*, 3290–3296.
- [5] a) N. W. Ockwig, O. Delgado-Friedrichs, M. O’Keeffe, O. M. Yaghi, *Acc. Chem. Res.* **2005**, *38*, 176–182; b) G. Férey, C. Serre, F. Millange, S. Surble, J. Dutour, I. Margiolaki, *Angew. Chem. Int. Ed.* **2004**, *43*, 6296–6301; *Angew. Chem.* **2004**, *116*, 6456–6461; c) Q. Fang, G. Zhu, M. Xue, J. Sun, Y. Wei, S. Qiu, R. Xu, *Angew. Chem. Int. Ed.* **2005**, *44*, 3845–3848; *Angew. Chem.* **2005**, *117*, 3913–3916; d) J. A. R. Navarro, E. Barea, J. M. Salas, N. Masciocchi, S. Galli, A. Sironi, C. O. Ania, J. B. Parra, *Inorg. Chem.* **2006**, *45*, 2397–2399; e) X. D. Guo, G. S. Zhu, Z. Y. Li, Y. Chen, X. T. Li, S. L. Qiu, *Inorg. Chem.* **2006**, *45*, 4065–4070; f) S. T. Zheng, F. Zuo, T. Wu, B. Irfanoglu, C. Chou, R. A. Nieto, P. Feng, X. Bu, *Angew. Chem. Int. Ed.* **2011**, *50*, 1849–1852; *Angew. Chem.* **2011**, *123*, 1889–1892.
- [6] a) Y. J. Cui, Y. F. Yue, G. D. Qian, B. L. Chen, *Chem. Rev.* **2012**, *112*, 1126–1162; b) L. E. Kreno, K. Leong, O. K. Farha, M. Allendorf, R. P. Van Duyne, J. T. Hupp, *Chem. Rev.* **2012**, *112*, 1105–1125; c) N. Yanai, K. Kitayama, Y. Hijikata, H. Sato, R. Matsuda, Y. Kubota, M. Takata, M. Mizuno, T. Uemura, S. Kitagawa, *Nat. Mater.* **2011**, *10*, 787–793.
- [7] a) Y. J. Cui, H. Xu, Y. F. Yue, Z. Y. Guo, G. D. Qian, B. L. Chen, *J. Am. Chem. Soc.* **2012**, *134*, 3979–3982; b) C. Y. Sun, X. L. Wang, X. Zhang, C. Qin, P. Li, Z. M. Su, J. Li, *Nat. Commun.* **2013**, *4*, 2717–2724; c) Y. J. Cui, T. Song, J. C. Yu, Y. Yang, Z. Y. Wang, G. D. Qian, *Adv. Funct. Mater.* **2015**, *25*, 4796–4802.
- [8] a) X. Z. Song, S. Y. Song, S. N. Zhao, Z. M. Hao, M. Zhu, X. Meng, L. L. Wu, H. J. Zhang, *Adv. Funct. Mater.* **2014**, *24*, 4034–4041; b) X. Zhao, X. Bu, T. Wu, S. T. Zheng, L. Wang, P. Feng, *Nat. Commun.* **2013**, *4*, 2344; c) N. B. Shustova, A. F. Cozzolino, S. Reineke, M. Baldo, M. Dincă, *J. Am. Chem. Soc.* **2013**, *135*, 13326–13329.
- [9] a) D. T. McQuade, A. E. Pullen, T. M. Swager, *Chem. Rev.* **2000**, *100*, 2537–2574; b) S. J. Toal, W. C. Trogler, *J. Mater. Chem.* **2006**, *16*, 2871–2883; c) M. E. Germain, M. J. Knapp, *Chem. Soc. Rev.* **2009**, *38*, 2543–2555.
- [10] Y. Takashima, V. M. Martínez, S. Furukawa, M. Kondo, S. Shimomura, H. Uehara, M. Nakahama, K. Sugimoto, S. Kitagawa, *Nat. Commun.* **2011**, *2*, 168–175.
- [11] a) B. Gole, A. K. Bar, P. S. Mukherjee, *Chem. Commun.* **2011**, *47*, 12137–12139; b) D. Tian, Y. Li, R. Y. Chen, Z. Chang, G. Y. Wang, X. H. Bu, *J. Mater. Chem. A* **2014**, *2*, 1465–1470; c) Y. Salinas, R. Martínez-Manez, M. D. Marcos, F. Sancenón, A. M. Castero, M. Parra, S. Gil, *Chem. Soc. Rev.* **2012**, *41*, 1261–1296.
- [12] a) E. Haque, V. Lo, A. I. Minett, A. T. Harris, T. L. Church, *J. Mater. Chem. A* **2014**, *2*, 193–203; b) C. Y. Sun, X. L. Wang, C. Qin, J. L. Jin, Z. M. Su, P. Huang, K. Z. Shao, *Chem. Eur. J.* **2013**, *19*, 3639–3645.
- [13] a) M. J. Dong, M. Zhao, S. Ou, C. Zou, C. D. Wu, *Angew. Chem. Int. Ed.* **2014**, *53*, 1575–1579; *Angew. Chem.* **2014**, *126*, 1601–1605; b) X. L. Hu, C. Qin, X. L. Wang, K. Z. Shao, Z. M. Su, *Chem. Commun.* **2015**, *51*,

- 17521–17524; c) S. N. Zhao, X. Z. Song, M. Zhu, X. Meng, L. L. Wu, J. Feng, S. Y. Song, H. J. Zhang, *Chem. Eur. J.* **2015**, *21*, 9748–9752.
- [14] a) J. Yu, Y. Cui, C. Wu, Y. Yang, Z. Wang, M. O'Keeffe, B. Chen, G. Qian, *Angew. Chem. Int. Ed.* **2012**, *51*, 10542–10545; *Angew. Chem.* **2012**, *124*, 10694–10697; b) H. He, E. Ma, Y. Cui, J. Yu, Y. Yang, T. Song, C. Wu, X. Chen, B. Chen, G. Qian, *Nat. Commun.* **2016**, *7*, 11087–11093; c) J. Yu, Y. Cui, H. Xu, Y. Yang, Z. Wang, B. Chen, G. Qian, *Nat. Commun.* **2013**, *4*, 2719–2725.
- [15] a) Y. Q. Lan, H. L. Jiang, S. L. Li, Q. Xu, *Adv. Mater.* **2011**, *23*, 5015–5020; b) W. Xie, W. W. He, D. Y. Du, S. L. Li, J. S. Qin, Z. M. Su, C. Y. Sun, Y. Q. Lan, *Chem. Commun.* **2016**, *52*, 3288–3291.
- [16] a) K. S. Park, Z. Ni, A. P. Côté, J. Y. Choi, R. Huang, F. J. Uribe-Romo, H. K. Chae, M. O'Keeffe, O. M. Yaghi, *Proc. Natl. Acad. Sci. USA* **2006**, *103*, 10186–10191; b) J. P. Zhang, Y. B. Zhang, J. B. Lin, X. M. Chen, *Chem. Rev.* **2012**, *112*, 1001–1033; c) N. F. Zheng, X. H. Bu, B. Wang, P. Y. Feng, *Science* **2002**, *298*, 2366–2369; d) M. O'Keeffe, M. Eddaoudi, H. Li, T. Reineke, O. M. Yaghi, *J. Solid State Chem.* **2000**, *152*, 3–20; e) Q. R. Fang, G. S. Zhu, M. Xue, J. Y. Sun, S. L. Qiu, *Dalton Trans.* **2006**, 2399–2402.
- [17] PLATON: A. L. Spek, *J. Appl. Crystallogr.* **2003**, *36*, 7–13.
- [18] a) J. T. Jia, F. X. Sun, T. Borjigin, H. Ren, T. T. Zhang, Z. Bian, L. X. Gao, G. S. Zhu, *Chem. Commun.* **2012**, *48*, 6010–6012; b) C. M. Doherty, Y. Gao, B. Marmiroli, H. Amenitsch, F. Lisi, L. Malfatti, K. Okada, M. Takahashi, A. J. Hill, P. Innocenzi, P. Falcaro, *J. Mater. Chem.* **2012**, *22*, 16191–16195; c) Y. C. He, J. Yang, W. Q. Kan, H. M. Zhang, Y. Y. Liu, J. F. Ma, *J. Mater. Chem. A* **2015**, *3*, 1675–1681.
- [19] J. R. Lakowicz, *Principles of Fluorescence Spectroscopy*, 3rd ed., Springer, Berlin, **2006**.
- [20] CCDC 1465369 contain the supplementary crystallographic data for this paper. These data are provided free of charge by The Cambridge Crystallographic Data Centre.

Received: July 24, 2016

Published online on October 14, 2016